EurJIC European Journal of Inorganic Chemistry

FULL PAPER

DOI: 10.1002/ejic.201101414

Coordination Chemistry of α-ω-Bis(pyridylimine) Ligands Containing Flexible Linkers with Copper(I)

Zhenzhong Hu,[a] Celine M. Schneider,[a,b] Christina N. Price,[a] Whitney M. Pye,[a] Louise N. Dawe,[a,c] and Francesca M. Kerton*[a]

Keywords: Supramolecular chemistry / Copper / N ligands / Coordination modes / Supercritical carbon dioxide

Copper(I) complexes of a series of six potentially tetradentate bis(pyridylimine) ligands were prepared, where the pyridylimine groups were separated by different linking units [in **L1**, $CH_2CH_2CH_2(SiMe_2O)_{20}SiMe_2CH_2CH_2CH_2$; in **L2**, $CH_2CH_2CH_2SiMe_2OSiMe_2CH_2CH_2CH_2$; in **L3**, CH_2CH_2; in **L4**, $CH_2(CH_2)_4CH_2$; in **L5**, $CH_2(CH_2)_7CH_2$; in **L6**, $CH_2CH_2CH_2OCH_2CH_2OCH_2CH_2OCH_2CH_2CH_2$]. The solubilities of **L1**, **L2** and [Cu(**L2**)](PF_6) in supercritical carbon dioxide were determined. The coordination chemistry of **L1**–**L2** with Cu^I was studied by UV/Vis, multinuclear NMR and IR spectroscopy, MALDI-TOF and ESI mass spectrometries and elemental analysis. These data suggested that [1+1] complexes had formed. Dicopper complexes of **L3**–**L6** were prepared for comparison, and $[Cu_2(\mathbf{L5})_2](PF_6)_2$ characterized by single-crystal X-ray diffraction analysis. Close methylene C–H···π interactions are observed within the structure. PGSE NMR spectroscopy was used to determine the hydrodynamic radii of the species in solution and comparison of these data with computational models for the complexes was made. Freezing point depression measurements afforded molecular weights for solution-state species in agreement with the formulations proposed via NMR and mass spectrometric data. There is no evidence to support linear metallopolymer formation but data suggest that [2+2] and [1+1] metallomacrocyles were formed, with siloxane linking groups encouraging the formation of [1+1] species. Solid-state NMR spectroscopic data on [Cu(**L1**)](PF_6) indicate the presence of two different environments for the PF_6^- anions.

Introduction

A number of research groups, including our own, have previously used mono end-capped polydimethylsiloxane (PDMS) in green chemistry and other applications,[1] including the preparation of CO_2-philic molecules with potential uses in green catalysis.[1a,1e,1f] Difunctional PDMS, containing ligating groups at either end of a PDMS chain, has been explored to a lesser extent in the field of coordination chemistry and catalysis. In such a situation, the ligands could bind to metal centres in a number of ways, Figure 1. Tritopic ligands separated by short PDMS chains have been used by Lehn and co-workers to prepare metal-containing extended polymers that can be processed into films with potential sensor applications.[2] Pyridylimine-based ligands have recently found applications in the field of catalytic water oxidation,[3] and have also been used extensively in olefin dimerization, oligomerization and polymerization catalysis.[4] We have recently used such ligands in catalytic aerobic oxidation reactions of alcohols.[5] Therefore, we decided to study their coordination chemistry in more detail to better understand catalytic reactions employing them and possible intermediates that might form.

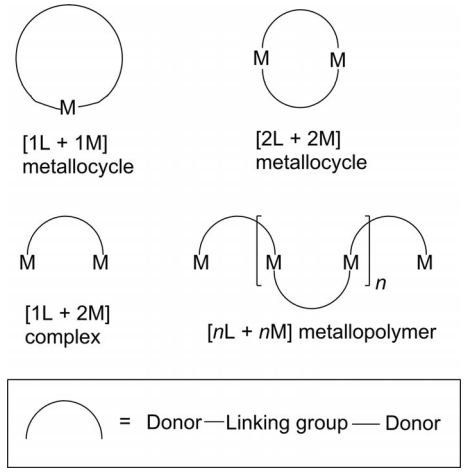

Figure 1. Schematic representation of possible binding modes for bridging/linked ligands.

[a] Department of Chemistry, Memorial University of Newfoundland,
St. John's, NL, A1B 3X7, Canada
Fax: +1-709-864-3702
E-mail: fkerton@mun.ca
[b] NMR Laboratory, Centre for Chemical Analysis, Research and Training, Memorial University of Newfoundland,
St. John's, NL, A1B 3X7, Canada
[c] X-ray Crystallography Laboratory, Centre for Chemical Analysis, Research and Training, Memorial University of Newfoundland,
St. John's, NL, A1B 3X7, Canada
Supporting information for this article is available on the WWW under http://dx.doi.org/10.1002/ejic.201101414.

Results and Discussion

The coordination chemistry of **L1**–**L6**, Figure 2, with copper(I) is described below. **L3** has been widely studied by others,[6] and was included in this work for comparative purposes.

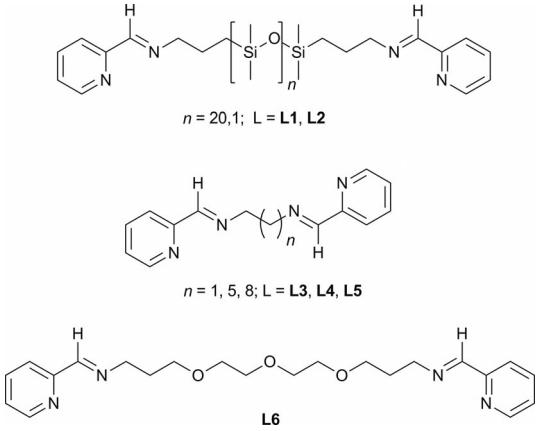

Figure 2. Ligands used in this study.

Preliminary Studies Using L1

As we had previously worked with PDMS-derived ligands,[1a] we studied the chemistry of **L1** first. The polymeric starting material PDMS-NH_2 and **L1** were characterized using ^{1}H NMR, ^{13}C{^{1}H} NMR, FT-IR, MALDI-TOF mass spectrometric (MS) data and elemental analyses. GPC analysis confirmed that no polymer degradation or coupling occurred during the synthesis of **L1** as its retention volume was nearly identical to PDMS-NH_2. The number of dimethylsiloxane repeat units (n) was determined using end-group analysis of the ^{1}H NMR spectrum and elemental analysis to be 20. It should be noted that increased relaxation times were used to obtain spectra where resonances could be integrated with greater accuracy. However, MS analysis revealed that **L1** had M_w 1567, M_n 1317 and a resulting polydispersity of 1.19. This corresponds to n = 16, but this low value could be a result of poor signal-to-noise ratio in the high mass region of the spectrum. Overall, the spectrum had a similar appearance to that of its coordination complex (see below and Supporting Information) in that the peak separations (74 mass units), their intensities and isotope patterns are typical for monodisperse PDMS chains.[7] Such monodisperse chains will have a narrow polydispersity (between 1.1 and 1.5), where polydispersity is the ratio of M_w/M_n (M_w = weight average molecular weight and gives greater statistical weighting to heavier molecules, M_n = number average molecular weight and gives greater statistical weighting to lighter molecules). When polydispersity is 1.0, all of the polymer chains will be of exactly the same weight and length.

In our previous studies, monodentate PDMS-derived ligands and their Pd complexes were found to be soluble in supercritical carbon dioxide ($scCO_2$).[1a] Therefore, the solubilities of **L1** and **L2** in $scCO_2$ were assessed. **L2** was miscible in liquid CO_2 at room temperature. Cloud point data for **L1** over the temperature range 60–100 °C were measured, Figure 3. Copper complexes of these ligands were prepared, see below, and their solubility in $scCO_2$ gauged. Significantly higher temperatures and pressures were needed to dissolve [Cu(**L2**)](PF_6) compared with the uncoordinated parent ligand **L2**, presumably due to the ionic nature of the metal complex. Unfortunately, [Cu(**L1**)](PF_6) was insoluble in CO_2 at all temperatures and pressures studied (25–120 °C, 4000–7500 psi).

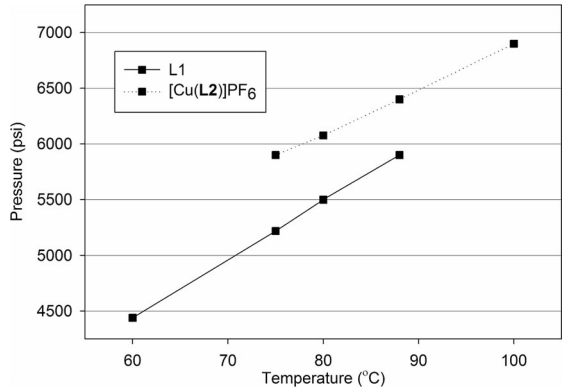

Figure 3. Cloud point data for **L1** and [Cu(**L2**)](PF_6), measurements made using a SFT phase monitor II.

Initial investigations into the coordination chemistry of **L1** were performed via UV/Vis spectroscopy, Figure 4. The spectra of [Cu(CH_3CN)$_4$](PF_6) and **L1** show no absorbances in the visible region. However, a MLCT band was seen to grow in intensity relative to an increase in concentration of copper(I) ions. This band reached a maximum intensity (λ = 465 nm, ε = 21 000 L mol^{-1} cm^{-1}) when there was one copper(I) ion per each **L1** corresponding to a [1+1] complex forming where each copper ion is surrounded by two chelating pyridylimine groups. This initial titration was performed in air but all further coordination chemistry experiments were performed under strictly air- and moisture-free conditions to avoid oxidation of the copper ion. The reaction was then performed on a synthetic scale and the resulting solid characterized using FT-IR, NMR, MALDI-TOF MS, GPC and elemental analyses. These data support the self-assembly of a [1+1] metallocyclopolymeric complex, [Cu(**L1**)](PF_6). The GPC chromatogram (using refractive index detection) contained a single, inverted peak at a retention volume nearly identical to **L1** and PDMS-NH_2. Due to the inversion of this peak (it appeared below the baseline of a control run as opposed to above it), mass data could not be obtained through conventional calibration against polystyrene standards. However, in contrast to previously characterized [1+1] metallocyclopolymers,[8] MS analyses show no evidence for larger [2+2] or other species. MALDI-TOF MS data, Table 1, revealed that the [Cu(**L1**)]$^+$ cations had M_w 1710, M_n 1382 and a polydispersity of 1.24. Modeling of ESI MS data also supported this for-

mulation. On comparing the M_n values of the complex ion with the free ligand **L1**, a difference of 65 mass units is obtained that is close to the molecular weight of Cu. Also, inspection of individual peaks within the mass spectrum showed an isotopic match corresponding to the presence of one copper atom and not two per polymer chain. However, at this stage, we could not overlook the possibility of either a gas-phase rearrangement/fragmentation within the mass spectrometer or the possibility of equilibration to yield the [1+1] complex from larger [*n*+*n*] species in solution during chromatographic analysis. We were intrigued by these results because, as far as we are aware, there are very few examples of [1+1] metallocycles,[8–9] and if the ligands are separated by flexible, long bridging groups, there is a tendency for mixtures to form.

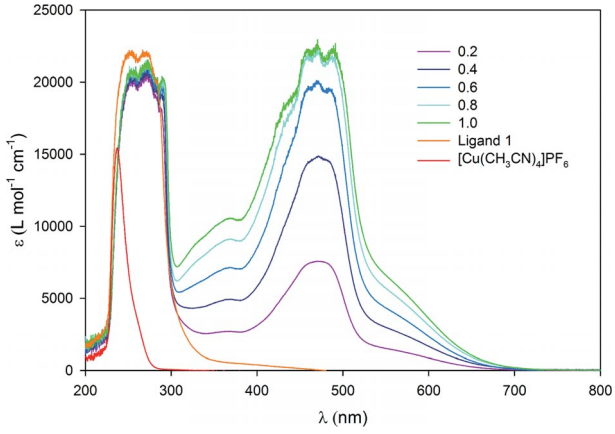

Figure 4. UV/Vis spectra for the titration of **L1** with $[Cu(CH_3CN)_4](PF_6)$ in CH_2Cl_2; Cu = $[Cu(CH_3CN)_4](PF_6)$ only, L1 = **L1** only, molar equiv. of Cu with respect to **L1** from 0.2 to 1.0.

Table 1. Comparison of mass data for complexes of **L1**, **L2** and **L5**.[a]

Complexes	Theoretical M_w	M_w from freezing point depression	M_w from MS
$[Cu(\mathbf{L1})]^+$	1895.5[b]	1740	M_w 1710 M_n 1382 (MALDI)
$[Cu(\mathbf{L2})]^+$	489.2	540[c]	489.3 (MALDI) 489.2 (ESI)
$[Cu_2(\mathbf{L5})_2]^{2+}$	798.3	980	943.3(MALDI)

[a] Data obtained for PF_6^- species unless otherwise indicated, (PF_6^- = 145.0 g mol^{-1}). [b] Exact mass value, $[Cu_2(\mathbf{L1})_2]^{2+}$ M_w = 3791. [c] BF_4^- complex (BF_4^- = 86.8 g mol^{-1}).

Preliminary Studies Using L2 as a Low Molecular Weight Model of L1

Due to the scarcity of well-characterized [1+1] complexes,[8–9] we undertook the synthesis of a low molecular weight analog using **L2**. Spectral data for the resulting compound agreed with the formulation $[Cu(\mathbf{L2})](PF_6)$. For example, the mass spectrum (positive mode) contained a single peak at an *m*/*z* and isotope match corresponding to [Cu + **L2**]$^+$, Table 1. Furthermore, UV/Vis analysis showed a MLCT band at 475 nm (ε = 16 000 L mol^{-1} cm^{-1}). The frequency of this absorbance is similar to that reported for the known dicopper(I) helicate complexes of **L3**,[10] but the molar extinction coefficient for the MLCT of the **L1** and **L2** complexes is much greater. The presence and energy of the MLCT band is in good agreement with the calculated energies of the frontier orbitals for $[Cu(\mathbf{L2})](PF_6)$ (Supporting Information). FT-IR data for our complexes are similar to structurally verified copper(I) and nickel(II) complexes of bidentate and tetradentate pyridylimine ligands.[6g,6j,11] However, both the electronic and vibrational spectroscopic data would be alike for [1+1] and [2+2] species. ^{1}H and ^{13}C solution NMR spectroscopic data for $[Cu(\mathbf{L1})](PF_6)$ and $[Cu(\mathbf{L2})](PF_6)$ show the expected number of resonances, which are moderately shifted compared to the free ligands. ^{1}H-^{1}H coupling observable for the pyridyl protons in the free ligand was not observed in the complexes presumably due to the fluxionality of coordinate covalent bonds in solution leading to signal broadening. Through parallels with known copper(I) pyridylimine complexes,[6a,6i,12] processes including inter- and intramolecular ligand exchange through twisting at the metal or ligand dissociation are thought to occur. Oxidation of the copper centre might also be the cause of signal broadening in these NMR spectra. However, EPR spectra of these samples were silent and gave no indication of the presence of copper(II).

Discussion of Mass Spectrometric Data for Copper(I) Complexes of L1–L6

L3–**L6** were prepared and their reactions with $[Cu(CH_3CN)_4](PF_6)$ investigated in order to obtain greater insight into the chemistry of **L1** and **L2**. **L4** has been explored to some extent previously,[13] and **L3** studied extensively by other chemists.[6] $[Cu_2(\mathbf{L3})_2](PF_6)_2$ and $[Cu_2(\mathbf{L3})_2](ClO_4)_2$ have been structurally characterized.[6i,6j] The central dicopper(I) helicate cation was determined to be 13.7 Å in diameter. A [1L + 2Cu] complex, $[Cu_2(\mathbf{L3})(PPh_3)_2I_2]$, has also been structurally characterized.[6f] An extensive study of copper complexes of **L3** and related ligands has been performed by Fabbrizzi and co-workers involving spectroelectrochemistry and mass spectrometric monitoring of the assembly and disassembly of the copper helicates.[10] They propose the formation of $[Cu^I(L)]^+$ complexes upon reduction of the analogous copper(II) ion and prior to the self-assembly of the typical copper(I) bimetallic bis(ligand) helicates. The lifetimes of the intermediate $[Cu^I(L)]^+$ species were assessed to be less than 20 ms, however, their presence in this cycle shows that the formation of such complexes is not thermodynamically barred rather that there is a kinetic preference for the helicate structures with these particular ligands.

In 1984, van Koten and co-workers reported extensive NMR studies on the dynamic behavior and solution-state structures of pyridylimine complexes of Ag^I and Cu^I including $[Cu_2(\mathbf{L3})_2](O_3SCF_3)_2$,[6a,12] using ^{1}H, natural-abundance INEPT ^{15}N and INEPT ^{109}Ag NMR experiments. Where

present the nature of the bridging C_2 chain between the pyridylimine ligands was determined to be the major influence on intramolecular fluxional processes.[6a] FD mass spectra for the complexes in that study confirmed the formation of dimetallic dications including $[Cu_2(\mathbf{L3})_2]^{2+}$. More recently, ESI mass spectra for $[Cu^{II}(\mathbf{L3})](CF_3SO_3)_2$ showed a peak at *m*/*z* 450 corresponding to $\{[Cu(\mathbf{L3})]CF_3SO_3\}^+$ and for $[Cu^{I}_2(\mathbf{L3})_2](ClO_4)_2$ showed a peak at *m*/*z* 701 corresponding to $\{[Cu_2(\mathbf{L3})_2]ClO_4\}^+$.[10] In ESI experiments performed in our laboratory, the mass spectrum for the copper(I) complex of **L3** contained a peak at *m*/*z* 747 corresponding to $\{[Cu_2(\mathbf{L3})_2]PF_6\}^+$. However, even with the fragmentor voltage set to low, all coordination compounds reported in this paper afforded spectra containing 100% intensity peaks which could be assigned to $[Cu + \mathbf{L}]^+$ on the basis of *m*/*z* and isotope patterns. It should be noted that $[Cu_2(\mathbf{L})_2]^{2+}$ species would appear at the same *m*/*z* positions as $[Cu + \mathbf{L}]^+$ ions but would possess significantly different isotope patterns. It should also be noted that care was taken to avoid oxidation of the copper(I) complexes in this study and therefore, the peaks in the mass spectra are not from copper(II) species. Furthermore, EPR spectra were silent strongly suggesting that copper(II) was not present. For **L2**, **L4**–**6**, ESI mass spectra showed no peaks that could be assigned to bimetallic species. Mass spectra for the polymeric ligand **L1** and its copper complex were discussed above. These data were obtained using a MALDI-TOF mass spectrometer. Therefore, we studied the complexes of **L2**–**L6** using this method. Using this type of ionization, bimetallic ions were observed for **L4**–**L6**. The molecular ion region of the mass spectra and theoretical isotope patterns for $\{[Cu_2(\mathbf{L})_2]PF_6\}^+$ (**L** = **L4**, **L5** or **L6**) are available in Supporting Information. Numerous MS spectra of **L1**–**L2** complexes were obtained but none showed evidence of bimetallic species. These results highlight that, if numerous related coordination complexes (monometallic, bimetallic, trimetallic etc.) could potentially be formed, it would be advisable to perform as broad a range of mass spectrometric experiments as possible to confirm initial results and data obtained using one technique.

Due to the range of different gas phase ions observed through mass spectrometry, freezing point depression experiments were performed in order to get solution phase values for comparison. Data from DMSO solutions of complexes are presented in Table 1 and show reasonable agreement with mass spectrometric-derived formulations.

PGSE NMR Studies of Copper(I) Complexes of L1–L6

In order to confirm the formation of the unusual large-sized [1+1] metallocyclic species $[Cu(\mathbf{L1})](PF_6)$ in solution, other analytical methods were pursued. Recently, Constable and co-workers have shown that Pulse-field gradient spin-echo (PGSE) NMR spectroscopy is a valuable technique to use in determining the size and, therefore, the major species in solution for $[Co_nL_n][PF_6]_{3n}$ metallomacrocyles.[14] PGSE diffusion NMR spectroscopy can be used to obtain diffusion coefficients of solution-state species and in turn this data can be used to obtain molecular sizes.[15] In the absence of structural data, and for comparison with NMR spectroscopic data, MMFF- and semi-empirical PM3-calculations were performed using SPARTAN '08 software to obtain approximate radii for the compounds in their geometry optimized equilibrium [1+1] and [2+2] forms (Figure 5 and Table 1). The relative stability of the two complexes was determined to be very similar and therefore, no conclusions regarding a thermodynamic preference for either form could be made.

The hydrodynamic radii, r_H, of the $[Cu_n\mathbf{L}_n]^{n+}$ species in solution were determined from the sample diffusion coefficients, *D*, Table 2, once a proper model (spherical model, ellipsoidal-prolate or ellipsoidal-oblate model) and equation had been chosen. Data from these diffusion studies, alongside computational studies, clearly suggest that **L1** and **L2** form [1+1] metal-ligand complexes. For $[Cu(\mathbf{L1})](PF_6)$, the experimentally determined radius from PGSE data was 13.7 ± 0.1 Å, which is much closer to the computationally modeled radius of the [1+1] complex (12.3 Å) than the [2+2] species (24.0 Å). The radius extracted from NMR spectroscopic data for copper(I) complexes with **L3** or **L5** showed reasonable agreement with that derived from X-ray diffraction data for the [2+2] species. For example, in solution $[Cu_2(\mathbf{L3})_2](PF_6)_2$ was determined to have a radius of 7.9 ± 0.1 Å from NMR spectro-

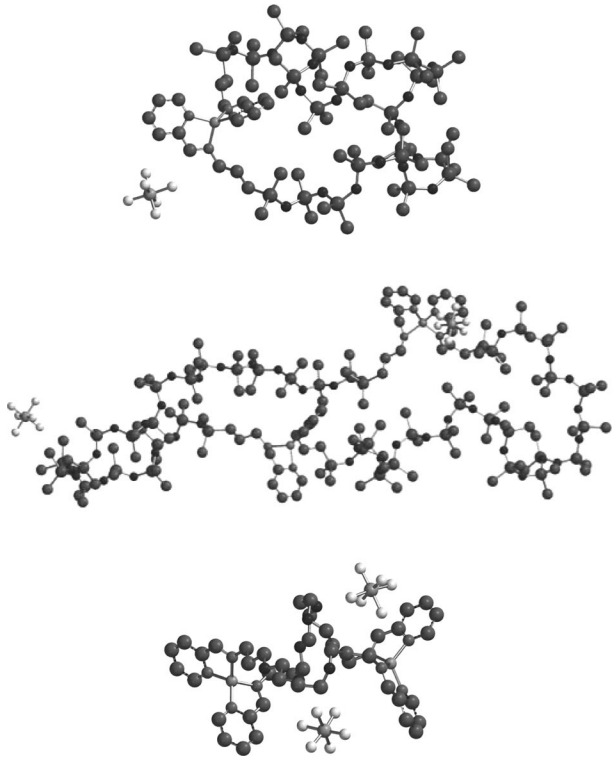

Figure 5. Molecular models of $[Cu_n(\mathbf{L1})_n](PF_6)_n$ (n = 1 and 2) and $[Cu_2(\mathbf{L6})_2](PF_6)_2$, obtained using SPARTAN '08 software [ground state equilibrium geometry, semi-empirical (restricted Hartree–Fock) PM3 calculation from an initial geometry obtained via MMFF calculation].

Table 2. Measured solution viscosity (η) and solution diffusion coefficients (D), calculated hydrodynamic radii, r_H, for copper coordination compounds and computationally modeled or known radii for [1+1] and [2+2] species.

Complexes	η [10^{-3} kg s^{-1} m^{-1}]	D [10^{-9} m^2 s^{-1}]	r_H [Å]	[1+1][a] [Å]	[2+2][a] [Å]
[Cu(**L1**)](PF$_6$)	0.70	0.54 ± 0.06	13.7 ± 0.1	12.3	24.0
[Cu(**L2**)](PF$_6$)	0.41	2.50 ± 0.12	4.1 ± 0.2	6.4	10.5
[Cu$_2$(**L2**)$_2$](BF$_4$)$_2$	0.29	3.44 ± 0.21	4.0 ± 0.5	6.4	10.5
[Cu$_2$(**L3**)$_2$](PF$_6$)$_2$	0.28	2.94 ± 0.06	7.9 ± 0.1	4.8	6.8[b]
[Cu$_2$(**L4**)$_2$](PF$_6$)$_2$	0.35	1.96 ± 0.07	9.6 ± 0.4	5.1	9.9
[Cu$_2$(**L5**)$_2$](PF$_6$)$_2$	0.38	1.18 ± 0.02	14.8 ± 0.3	5.6	10.5, 10.6[c]
[Cu$_2$(**L6**)$_2$](PF$_6$)$_2$	0.34	2.06 ± 0.25	9.7 ± 1.1	6.4	10.4

[a] Unless otherwise indicated, approximate radii for the compounds in their geometry optimized equilibrium forms obtained through MMFF- and semi-empirical PM3-calculations using SPARTAN '08 software. [b] The radius for [Cu$_2$(**L3**)$_2$]$^{2+}$ in the solid-state from crystallographic data reported in ref.[6i] [c] The radius of [Cu$_2$(**L5**)$_2$]$^{2+}$ in the solid-state from crystallographic data reported herein.

scopic data and in the solid-state it has been shown to have a radius of 6.8 Å. Also, hydrodynamic radii data and computational studies clearly suggest that **L4** and **L6** form bimetallic dicationic complexes in solution. Furthermore, the NMR-derived radii for the copper complexes with all ligands showed good agreement with the formulation determined from mass spectrometric evidence, Table 1 and Exp. Section.

X-ray Diffraction Data

Unfortunately to date, we have been unable to obtain single crystals of our model complex, [Cu(**L2**)](PF$_6$), to unambiguously confirm the cyclic [1+1] nature of the siloxane-containing complexes in the solid-state. However, over the course of our studies, we noticed that during solvent evaporation from solutions of [Cu(**L1**)](PF$_6$) dark-coloured seed crystals formed on the surface of the glassware. Upon further inspection under a microscope, these crystalline domains became more visible, especially under cross-polarized light (Supporting Information). At room temperature, powder X-ray diffraction analysis of [Cu(**L1**)](PF$_6$) showed two intense, sharp peaks at a constant Bragg angle 2θ of 0.42° and 1.44°. These correspond to d-spacings of 210.1 Å and 61.3 Å. Both are significantly longer than the predicted diameter of the metallocyclopolymer, which is calculated to be 24.6 Å for a [1+1] complex and 48.0 Å for a bimetallic [2+2] complex. Therefore, bimolecular (or greater) aggregration must exist within the crystalline phase. Recently, Gloe and co-workers reported the remarkable self-assembly of three hexametallic copper(II) *meso*-helicates, [CuL(SO$_4$)]$_6$·24H$_2$O where L is a linked bis-pyridylimine ligand, that were circular in shape.[16] The self-assembly was controlled by the coordination of sulfate ions with the copper(II) centres. The diameter of these structures in the solid-state was determined to be 31–32 Å by single-crystal X-ray diffraction analysis. At this stage, a multimetallic structure similar to these cannot be ruled out for the **L1** complex in the solid-state. Although, in solution and in the gas phase [1+1] species dominate, as discussed earlier. However, the crystalline nature of the complex does rule out a supramolecular linear metallopolymer, as by analogy to Lehn and Chow's results an elastomeric polymer would be expected due to the flexible nature of the PDMS linking group.[2]

Extensive efforts were made to grow and isolate crystals of the complexes reported herein. One sample of [Cu$_2$(**L5**)$_2$](PF$_6$)$_2$ upon storage at –20 °C in a methanol solution for over one year afforded brown crystals amenable to single-crystal X-ray diffraction analysis. The asymmetric unit contained two independent half complexes and two half-occupancy methanol molecules. Closer inspection of the coordination environment around copper reveals that Cu1–N2 is significantly shorter [1.770(7) Å; Figure 6] than the other Cu–N bond lengths [1.979(6)–2.068(8) Å]. The second molecule in the dimer contains typical Cu–N bond lengths for copper-imine and copper-pyridine interactions (Figure 7). This X-ray determined structure confirms the dimetallic nature of the **L5** species formed, which was proposed through mass spectrometric, PGSE NMR and freezing point depression data. Furthermore, the radius of the complex is in good agreement with that determined through PM3-calculations, Table 1.

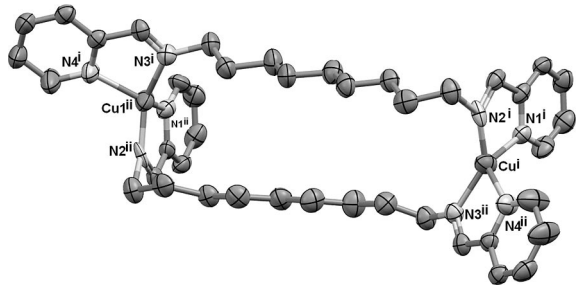

Figure 6. 30% probability ellipsoid representation of one of the two bimetallic moieties, {Cu$_2$(**L5**)$_2$} (H-atoms omitted for clarity). Symmetry codes: (i) x, y, z (ii) x, 1.25 – y, 1.25 – z. Selected bond lengths [Å] and bond angles [°]: Cu1–N2 1.770(7); Cu1–N3 1.983(7); Cu1–N4 2.062(8); Cu1–N1 2.069(8); Cu2–N7 1.979(6); Cu2–N6 1.990(7); Cu2–N5 2.047(8); Cu2–N8 2.054(7) N2–Cu1–N3 140.9(3); N2–Cu1–N4 113.0(3); N3–Cu1–N4 80.9(3); N2–Cu1–N1 83.6(3); N3–Cu1–N1 119.2(3); N4–Cu1–N1 125.1(3); N7–Cu2–N6 140.6(3); N7–Cu2–N5 118.0(3); N6–Cu2–N5 82.1(3); N7–Cu2–N8 82.2(3); N6–Cu2–N8 112.2(3); N5–Cu2–N8 129.4(3).

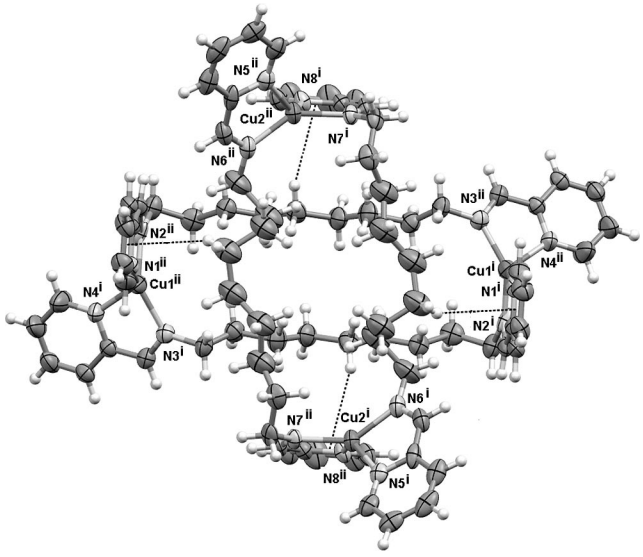

Figure 7. Dimer unit, $[Cu_2(\mathbf{L5})_2]_2$, showing close methylene C–H···π interactions (30% probability ellipsoids); disordered carbon-chain atoms, PF_6^- ions and lattice solvent CH_3OH omitted for clarity.

Each dimer [Figure 7; symmetry related atoms generated by (x, 1.25 – y, 1.25 – z)] is generated by the intersection of one twofold proper rotation axis and one twofold screw axis, with one molecule aligned lengthwise with the b axis, and the other with the c axis. Very close intermolecular methylene C–H···π interactions are present, with C11–H11B···Cg1 3.07 Å and C31–H31B···Cg2 2.94 Å [where Cg1 and Cg2 are the centroids of the rings formed by (N8, C38-C42) and (N1, C1–C5), respectively; these are indicated by dashed lines in Figure 7]. Such C–H···π interactions may in part be the cause of the different formulation observed for copper complexes of the siloxane-derived ligands, as the –$OSiMe_2$– linkers would not facilitate this phenomenon. The unit cell contains 16 solvent accessible volumes (each measuring 181–182 Å^3) that run parallel to the c-axis, centered with average x and y positions given by (nx/8, my/8) (where n and m = 1, 3, 5, 7; these lie on twofold proper rotation axes), occupied by disordered methanol molecules (Figure 8; solvent and H-atoms omitted for clarity). The model contains 32 methanol molecules per unit cell; that is, two methanol molecules are contained in each void, consistent with the maximum number of expected methanol molecules based on their volume in the liquid phase (ca. 67.2 Å^3).

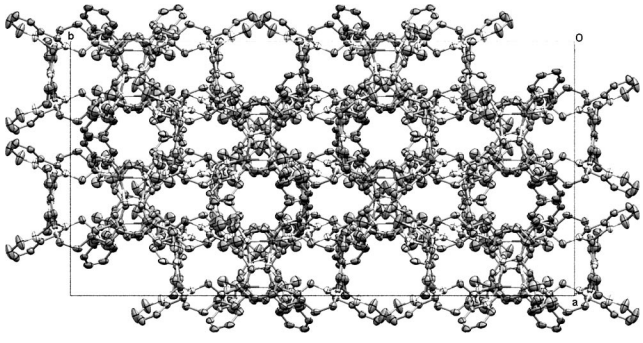

Figure 8. Packed unit cell, viewed down the c axis. H-atoms, disordered carbon-chain atoms, PF_6^- ions and lattice solvent CH_3OH omitted for clarity.

Solid-State NMR Studies

In an attempt to confirm the presence of cyclic species in the solid-state, MAS NMR experiments were performed [Cu(**L1**)](PF_6) and [Cu(**L2**)](PF_6), Figure 9. As a baseline for comparison, data was also obtained for [$Cu(CH_3CN)_4$](PF_6), see Supporting Information. The ^{19}F NMR spectrum in solution exhibits a doublet at δ = –75 ppm, $J_{P,F}$ = 711 Hz with a relaxation time T_2* of 72.0 ms. In the solid-state, the signal shifts to higher frequency, –67 ppm, $J_{P,F}$ remains unchanged and T_2* decreases to 2.0 ms. T_2* relaxation times are a reflection of the mobility (or tumbling) of the nucleus. Therefore, values in solution are typically much larger than solid-state values. The solid-state ^{31}P NMR spectrum of [$Cu(CH_3CN)_4$](PF_6) exhibits a sept at δ = –142 ppm, $J_{P,F}$ = 709 Hz and T_2* of 5.2 ms. This frequency and coupling constant is typical for a non-constrained hexafluorophosphate anion in the solid-state.[17] ^{19}F NMR spectra of [Cu(**L1**)](PF_6) and [Cu(**L2**)](PF_6) in solution display the expected doublet resonance (Supporting Information), but in the solid state [Cu(**L1**)](PF_6) is significantly different to the other species studied. The relaxation time for the ^{31}P environment is significantly shorter for the **L1** complex (0.34 ms) compared with the **L2** complex (1.26 ms) and [$Cu(CH_3CN)_4$](PF_6) (5.2 ms). This leads to significant broadening of the resonances for the **L1** species. The dramatically shorter T_2* and T_2 values suggest that the anions are held in a much more rigid environment in the cyclopolymer complex. Furthermore, for [Cu(**L1**)](PF_6) the broad

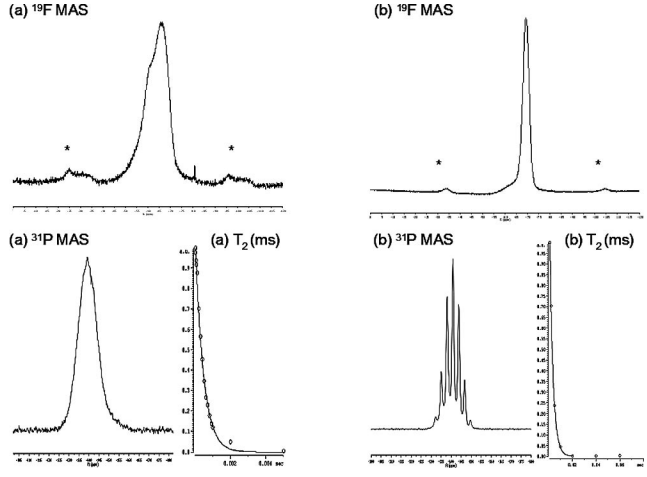

Figure 9. Solid-state NMR spectra for (a) [Cu(**L1**)](PF_6), ^{19}F-NMR δ = –65 (v. br.) (deconvoluted as two environments) δ = –67 (F1 35%), –60 (F2 65%), ^{31}P-NMR: δ = –139 (v. br.), J_{F-P} = 685 Hz, T_2 = 0.46 ms, T_2* = 0.34 ms; (b) [Cu(**L2**)](PF_6), ^{19}F-NMR δ = –70 (br.), ^{31}P-NMR δ = –141 (sept), J_{F-P} = 711 Hz, T_2 = 2.81 ms, T_2* = 1.26 ms (*: spinning side bands).

^{19}F resonance, –65 ppm, can be modeled as two ^{19}F environments, –67 and –60 ppm, with occupancies of 35% and 65% respectively. These unusual differences in NMR spectroscopic data could be interpreted in a number of ways. We tentatively propose that in [Cu(**L1**)](PF_6) some of the anions are held within cyclic or cage structures like a metal ion within a crown ether and therefore, have restricted motion compared with the small molecule **L2** analog where the anion cannot fit inside the macrocycle or cage. Hydrolysis of the PF_6^- anion or oxidation of the copper ion were ruled out as the reasons for the signal broadening and the presence of two environments in the ^{19}F MAS NMR spectrum, because (i) if the same sample is dissolved and solution NMR spectroscopic data is obtained a single environment is observed, and (ii) ESI MS showed no evidence of PF_6^- hydrolysis or copper oxidation ($z = 2$ ions should be evident if oxidation occurred). Also, EPR spectra were silent.

Conclusions

In summary, we have found that chelating pyridylimine ligands separated by a low molecular weight dimethylsiloxane or polymeric PDMS group can form [1+1] metallocycles. We tentatively propose that this is due to their inability to undergo C–H···π interactions due to their increased steric demand compared with $–(CH_2)_n–$ and $–(CH_2O)_n–$ bridging units. Some of the siloxane-derived compounds are soluble in $scCO_2$. PGSE NMR spectroscopy was useful in ascertaining the size of these and related complexes in solution and in confirming the formation of [1+1] or [2+2] species suggested from mass spectrometric data. For **L5**, crystals were grown and X-ray diffraction analysis confirmed its [2+2] nature. The extended structure of this complex exhibited interesting packing in the solid-state. Solid-state ^{19}F NMR spectroscopic data for the polymeric metallocycle (**L1** complex) suggests two environments exist for the hexafluorophosphate anion. We propose that the anion could reside both inside and outside a cycle or cavity, which is feasible given the size and resulting cavity in the proposed [1+1] species.

Experimental Section

General Information: All reactions were carried out under dry nitrogen using standard Schlenk-line techniques. THF was dried and distilled from sodium benzophenone ketyl, whilst CH_2Cl_2 was dried and distilled from CaH_2. 2-Pyridinecarbaldehyde, tetrakis(acetonitrile)copper(I) hexafluorophosphate and other reagents unless specified were purchased from Aldrich and used as received. PDMS-NH_2 [$H_2N(CH_2)_3(SiMe_2O)_{20}SiMe_2(CH_2)_3NH_2$] and 1,3-Bis(aminopropyl)tetramethyldisiloxane were purchased from Gelest. The ligands **L1**–**L6** were prepared as described previously.[5] Elemental analyses were performed by Canadian Microanalytical Service Ltd. (Delta, BC). ^1H-NMR spectra were acquired on a Bruker AVANCE 500 MHz spectrometer. $^{13}C\{^1H\}$-, ^{19}F- and ^{31}P-NMR spectra were acquired on a Bruker AVANCE 300 MHz spectrometer. ^{19}F-NMR and ^{31}P-NMR solid-state (and some solution) spectra were acquired on a Bruker AVANCE II 600 MHz spectrometer. Chemical shifts were reported in ppm using the residual protons of the deuterated free $CDCl_3$ or tetramethylsilane as an internal reference. Tetramethylsilane-free deuterated solvents were used in the collection of NMR spectra for all siloxane containing species. For polymeric samples in solution, delays were increased to allow complete relaxation of all protons and to obtain more accurate integration. For **L1**, **L2** and their copper complexes, MALDI-TOF mass spectroscopic data were obtained using an Applied Biosystems Voyager mass spectrometer. Dithranol was used as the matrix. For copper complexes of **L2**, **L4**–**L6**, mass spectroscopic data were obtained using an ABI QSTAR XL (Applied Biosystems/MDS Scies, Foster City, USA) hybrid quadrupole TOF MS/MS system equipped with an oMALDI 2 ion source. Dihydroxybenzoic acid (DHB) was used as the matrix. Also, for copper complexes of **L1**–**L6**, ESI-MS spectra were recorded using direct injection into an Agilent 1100 LC/MSD (G1946A) instrument in ESI mode (solvent: acetonitrile, concentration: 1 mg/mL). The capillary voltage of the instrument was 3000 V and the fragmentor voltage was varied through low, medium and high settings for all samples. X-ray Powder Diffraction data were obtained on a Rigaku Ru-200 12 kW Automated Powder Diffractometer. Polarized microphotos were obtained using a Leica DM 2500 microscope. A Bruker TENSOR 27 spectrometer was used to record FT-IR spectra. Gel permeation chromatographs (GPC) were obtained using a Viscotek VE 2001 instrument equipped with RI detector using the following condition: column type: Poly[Analytik]n, PAS-106M-H, 8.0 mm (ID) × 300 mm (L); flow rate: 1.0 mL/min; solvent: chlorobenzene. UV/Vis spectra were recorded using an Ocean Optics UV/Vis spectrometer. TGA spectra were measured by Universal V4.5A TA instrument. Solubility studies on ligands and complexes in supercritical carbon dioxide were performed using a Supercritical Fluids Technologies Phase Monitor II (SFT PM II). Freezing point depression measurements were obtained using a LabQuest data acquisition unit, a temperature probe and solutions of the copper complexes in DMSO (HPLC grade). Homogeneous solutions were prepared by heating the metal complexes in DMSO at 36 °C overnight and measurements made while slowly cooling the solutions in an ice salt bath. Using benzophenone as a standard, K_f (the molal freezing point constant) for DMSO was determined to be 4.20 K mol^{-1} kg. EPR experiments were performed on a Magnettech benchtop EPR spectrometer MiniScope MS100.

Computational Studies: Molecular model structures were obtained using SPARTAN '08 software [ground state equilibrium geometries, semi-empirical (restricted Hartree–Fock) PM3 calculations from initial geometries obtained via MMFF calculations]. Using SPARTAN '06 software, a higher level calculation was performed on [Cu(**L2**)]PF_6 (a restricted hybrid HF-DFT SCF calculation performed using Pulay DIIS + Geometric Direct Minimization, Method: RB3LYP, Basis set: 6-31G(D). Images representing the frontier orbitals in this molecule are presented in the Supporting Information.

Crystallographic Procedures: A crystal of [Cu_2(**L5**)$_2$](PF_6)$_2$·CH_3OH was mounted on a low temperature diffraction loop and measured on a Rigaku Saturn CCD area detector with graphite monochromated Mo-K_α radiation (Table 3). The structure was solved by direct methods[19a] and expanded using Fourier techniques.[19b] Neutral atom scattering factors were taken from Cromer and Waber.[19c] Anomalous dispersion effects were included in F_{calc};[19d] the values for $\Delta f'$ and $\Delta f''$ were those of Creagh and McAuley[19e] The values for the mass attenuation coefficients are those of Creagh and Hubbell.[19f] All calculations were performed using CrystalStructure[19g,19h] except for refinement, which was performed using SHELXL-97.[19a] All non-hydrogen atoms were refined anisotropi-

cally, however, DFIX and SIMU restraints were used to model the disordered chain [PART 1 C30-C32 and corresponding protons, 0.448(12) occupancy, PART 2 C30A-C32A and corresponding protons, 0.552(12) occupancy]. All H-atoms were introduced in calculated positions and refined on a riding model.

Table 3. Summary of crystal data for $\{[Cu_2(\mathbf{L5})_2](PF_6)_2\}_2$.

Compound reference	$[Cu_2(\mathbf{L5})_2](PF_6)_2{\cdot}CH_3OH$
Chemical formula	$C_{43}H_{60}Cu_2F_{12}N_8OP_2$
Formula mass	1122.02
Crystal system	orthorhombic
a /Å	20.339(5)
b /Å	40.0583(10)
c /Å	51.004(12)
α /°	90.00
β /°	90.00
γ /°	90.00
Unit cell volume /Å^3	41555(14)
Temperature /K	163(2)
Space group	*Fddd*
Z	32
Radiation type	Mo-K_α
Absorption coefficient, μ /mm^{-1}	0.964
Reflections measured	73518
Independent reflections	7695
R_{int}	0.0558
Final R_1 [$I > 2\sigma(I)$]	0.1117
Final $wR(F^2)$ (all data)	0.3282
GOF on F^2	1.149

CCDC-857548 (for copper complex of **L5**) contains the supplementary crystallographic data for this paper. These data can be obtained free of charge from The Cambridge Crystallographic Data Centre via www.ccdc.cam.ac.uk/data_request/cif.

General Procedure for Preparation of Cu^I Complexes: $[Cu(\mathbf{L1})](PF_6)$, $[Cu(\mathbf{L2})](PF_6)$, $[Cu(\mathbf{L2})](BF_4)$, $[Cu_2(\mathbf{L3})_2](PF_6)_2$, $[Cu_2(\mathbf{L4})_2](PF_6)_2$, $[Cu_2(\mathbf{L5})_2](PF_6)_2$, $[Cu_2(\mathbf{L6})_2](PF_6)_2$.

For [Cu(L1)]PF$_6$: Tetrakis(acetonitrile)copper(I) hexafluorophosphate (0.744 g, 2.00 mmol) was added to a Schlenk flask containing THF (50 mL). This mixture was left to stir until all of the copper salt had dissolved. **L1** (3.64 g, ca. 2.0 mmol) was dissolved in THF (5 mL) and transferred to the flask containing the copper salt via cannula. The dark red solution was stirred at room temperature for 24 h. The solvent was removed under vacuum and the product was isolated as a dark red-brown sticky solid; yield 52%.

For the remaining complexes, reactions were performed in CH_2Cl_2 and stirred at room temperature for 12 h. $[Cu(\mathbf{L2})]PF_6$, $[Cu(\mathbf{L2})]BF_4$, $[Cu_2(\mathbf{L3})_2](PF_6)_2$, $[Cu_2(\mathbf{L4})_2](PF_6)_2$ and $[Cu_2(\mathbf{L5})_2](PF_6)_2$, were isolated as dark red-brown powders; yields 83–88%. $[Cu_2(\mathbf{L6})_2](PF_6)_2$ was isolated as a dark brown powder; yield 90%.

[Cu(L1)]PF$_6$: ^{1}H NMR (500 MHz, $CDCl_3$, 298 K): δ = 8.61 (s, 2 H), 8.44 (s, 2 H), 8.01 (s, 2 H), 7.89 (s, 2 H), 7.58 (s, 2 H), 3.80 (s, 4 H), 1.67 (s, 4 H), 0.53 (s, 4 H), –0.05 to +0.08 (br., 126 H) ppm. ^{19}F NMR (565 MHz, solid state, 298 K): δ = –61, –67 ppm. ^{31}P NMR (243 MHz, solid state, 298 K): δ = –140 (v.br.) ppm. IR (KBr): $\tilde{\nu}$ = 2963, 2359, 1592, 1437, 1301, 1258, 1017, 835, 793, 705, 668 cm^{-1}. MS (MALDI-TOF, matrix: dithranol): *Mw* = 1710, *Mn* = 1382, polydispersity 1.24; found C 35.10, H 7.01, N 2.91. $C_{60}H_{148}N_4O_{20}Si_{21}CuPF_6$ requires C 35.25, H 7.30, N 2.74%.

[Cu(L2)]PF$_6$: ^{1}H NMR (500 MHz, $CDCl_3$, 298 K): δ = 8.59 (s, 2 H), 8.38 (s, 2 H), 8.01 (s, 2 H), 7.88 (s, 2 H), 7.59 (s, 2 H), 3.84 (s, 4 H), 1.81 (s, 4 H), 0.42 (s, 4 H), 0.02 (s, 12 H) ppm. ^{13}C{^{1}H} NMR (75 MHz, $CDCl_3$, 298 K): δ = 161.3, 150.7, 148.7, 138.5, 128.0, 127.2, 63.6, 24.9, 15.3, 0.4 ppm. ^{19}F NMR (565 MHz, solid state, 298 K): δ = –70 (br.) ppm. ^{31}P NMR (243 MHz, solid state, 298 K): δ = –141 (sept, $J_{F\text{-}P}$ = 711 Hz) ppm. IR (KBr): $\tilde{\nu}$ = 2954, 1594, 1443, 1265, 1058, 843, 772, 734, 703 cm^{-1}. MALDI-TOF MS (matrix: dithranol or dihydroxybenzoic acid): *m*/*z* 489.3 [**L2** + Cu$^+$]. ESI MS (CH_3CN): *m*/*z* 489.2 (100) [**L2** + Cu$^+$]; found C 41.22, H 5.29, N 8.54. $C_{22}H_{34}N_4OSi_2CuPF_6$ requires C 41.60, H 5.40, N 8.82%.

[Cu(L2)]BF$_4$: ^{1}H NMR (500 MHz, $CDCl_3$, 298 K): δ = 8.59 (s, 2 H), 8.39 (s, 2 H), 8.01 (s, 2 H), 7.87 (s, 2 H), 7.58 (s, 2 H), 3.84 (s, 4 H), 1.81 (s, 4 H), 0.41 (s, 4 H), 0.03 (s, 12 H) ppm. ^{13}C{^{1}H}NMR (75 MHz, $CDCl_3$, 298 K): δ = 161.3, 150.7, 148.7, 138.5, 128.0, 127.2, 77.6, 77.2, 76.7, 63.6, 24.9, 15.3, 0.4 ppm. MALDI-TOF MS (matrix: dihydroxybenzoic acid): *m*/*z* 489.3 [**L2** + Cu$^+$]. ESI MS (CH_3CN): *m*/*z* 489.2 (100) [**L2** + Cu$^+$]; found C 45.97, H 5.87, N 9.48. $C_{22}H_{34}N_4OSi_2CuBF_4$ requires C 45.79, H 5.94, N 9.71%.

[Cu$_2$(L4)$_2$](PF$_6$)$_2$: ^{1}H NMR (500 MHz, CD_3CN, 298 K): δ = 8.58 (s, 2 H), 8.37 (s, 2 H), 8.07 (s, 2 H), 7.81 (s, 2 H), 7.62 (s, 2 H), 3.73 (s, 4 H), 1.57 (s, 2 H), 1.19 (s, 2 H) ppm. ^{13}C{^{1}H} NMR (75 MHz, [D$_6$]acetone, 298 K): δ = 162.6, 151.8, 150.0, 139.5, 129.1, 127.8, 60.4, 31.8, 27.4 ppm. ^{19}F NMR (282 MHz, [D$_6$]acetone, 298 K): δ = –73.00 (d, $J_{F\text{-}P}$ = 708 Hz) ppm. ^{31}P NMR (122 MHz, [D$_6$]acetone, 298 K): δ = –144.1 (sept, $J_{F\text{-}P}$ = 708 Hz) ppm. IR (KBr): $\tilde{\nu}$ = 2928, 2857, 1592, 1441, 1302, 1254, 1157, 828, 770 cm^{-1}. MALDI-TOF MS (matrix: dihydroxybenzoic acid): *m*/*z* 859.2 [2**L4** + 2Cu + PF$_6$]$^+$. ESI MS (CH_3CN): *m*/*z* 357.4 (100) [**L4** + Cu]$^+$; found C 42.71, H 4.35, N 10.97. $C_{18}H_{22}N_4CuPF_6$ requires C 42.99, H 4.41, N 11.14%.

[Cu$_2$(L5)$_2$](PF$_6$)$_2$: ^{1}H NMR (500 MHz, [D$_6$]acetone, 298 K): δ = 8.91 (s, 2 H), 8.62 (s, 2 H), 8.23 (s, 2 H), 8.07 (s, 2 H), 7.78 (s, 2 H), 3.91 (s, 4 H), 1.71 (s, 4 H), 1.48–0.78 (m, 10 H) ppm. ^{13}C{^{1}H} NMR (75 MHz, [D$_6$]acetone, 298 K): δ = 162.5, 151.9, 150.1, 139.5, 129.2, 127.9, 60.7, 31.8, 27.7 ppm. ^{19}F NMR (282 MHz, [D$_6$]acetone, 298 K): δ = –72.33 (d, $J_{F\text{-}P}$ = 708 Hz) ppm. ^{31}P NMR (122 MHz, [D$_6$]acetone, 298 K): δ = –144.1 (sept, $J_{F\text{-}P}$ = 708 Hz) ppm. IR (KBr): $\tilde{\nu}$ = 2925, 2854, 1592, 1466, 1441, 1302, 1218, 1154, 830, 771 cm^{-1}. MALDI-TOF MS (matrix: dihydroxybenzoic acid): *m*/*z* 943.3 [2**L5** + 2Cu + PF$_6$]$^+$. ESI MS (CH_3CN): *m*/*z* 399.5 (100) [**L5** + Cu]$^+$; found C 45.84, H 5.07, N 10.59. $C_{21}H_{28}N_4CuPF_6$ requires C 46.28, H 5.18, N 10.28%.

[Cu$_2$(L6)$_2$](PF$_6$)$_2$: ^{1}H NMR (500 MHz, CD_3CN, 298 K): δ = 8.66 (s, 2 H), 8.46 (s, 2 H), 8.09 (s, 2 H), 7.88 (s, 2 H), 7.66 (s, 2 H), 3.89 (s, 4 H), 3.43 (s, 8 H), 3.37 (s, 4 H), 1.85 (s, 4 H ppm.) ^{13}C{^{1}H} NMR (75 MHz, CD_3CN, 298 K): δ = 162.5, 151.9, 150.0, 139.3, 129.1, 127.7, 71.4, 70.5, 68.5, 57.6, 31.7 ppm. ^{19}F NMR (282 MHz, CD_3CN, 298 K): δ = –72.71 (d, $J_{F\text{-}P}$ = 707 Hz) ppm. ^{31}P NMR (243 MHz, CD_3CN, 298 K): δ = –144.5 (sept, $J_{F\text{-}P}$ = 707 Hz) ppm. IR (KBr): $\tilde{\nu}$ = 2862, 1592, 1466, 1444, 1301, 1260, 1099, 828, 771 cm^{-1}. MALDI-TOF MS (matrix: dihydroxybenzoic acid): *m*/*z* 1067.3 [2**L6** + 2Cu + PF$_6$]$^+$. ESI-MS (CH_3CN): *m*/*z* 461.4 (100) [**L6** + Cu]$^+$; found C 43.75, H 4.81, N 9.07. $C_{22}H_{30}N_4O_3CuPF_6$ requires C 43.53, H 4.98, N 9.23%.

PGSE NMR Spectroscopy: Diffusion NMR measurements were performed on a Bruker Avance II 600 NMR spectrometer equipped with a 5-mm TXI probe and a *z*-gradient coil with a maximum strength of 5.35 G cm^{-1} at 298 K. Samples were run in $CDCl_3$ and in CD_3CN. The 90° pulse lengths were determined for each sample. A standard 2D sequence with stimulated echo and spoil gradient (STEGP) was used. A gradient recovery delay of 2 ms was used and the relaxation delay was set at 10 s. The gradient strength was calibrated by using the self-diffusion coefficient of residual HOD

in D_2O ($1.9\ 10^{-9}\ m^2s^{-1}$). For each experiment, the gradient strength was increased from 2–95% in 32 equally spaced steps with 16 scans per increment. Values of *d* (gradient pulse length) and *D* (diffusion time) were optimized on the sample HU-1 (coordination complex of **L1**) to give an intensity of between 5 and 10% of the initial intensity at 95% gradient strength and were set to 1.5 ms and 100 ms respectively for all subsequent samples.

The solvent peak was used as an internal standard to measure the viscosity of each sample. To that end, the diffusion coefficient of the pure solvent ($CDCl_3$ and CD_3CN) was first measured. This diffusion coefficient D_0 corresponds to the known viscosity η_0 of the pure solvent according to the Stokes–Einstein Equation (1).

$$D_0 = \frac{kT}{Br\eta_0} \quad (1)$$

Therefore for the solvent peak the diffusion coefficient in solution, D_{sol}, is afforded by Equation (2).

$$D_{sol} = \frac{kT}{Br\eta_{sol}} \quad (2)$$

Consequently the viscosity of each solution is obtained from Equation (3).

$$\eta_{sol} = \frac{D_0}{D_{sol}}\eta_0 \quad (3)$$

The numerical coefficient B has been shown to vary from 2 to 6π,[18] and can be calculated from the pure solvent diffusion coefficient too.

The data were plotted using MestReNova as Peak area vs. $Q = g^2\delta^2G^2(\Delta - \delta/3)$ and the diffusion coefficient (*D*) was extracted by fitting a mono exponential function [$I = I^0\exp(-D^*Q)$] with the data analysis component of the software.

Supporting Information (see footnote on the first page of this article): Geometry optimized structure and frontier orbitals of [Cu(**L2**)](PF_6), mass spectra of $[Cu_n(\mathbf{L})_n](PF_6)_n$ complexes, UV/Vis spectrum of [Cu(**L2**)](PF_6), IR spectra of PDMS-NH_2, **L1** and [Cu(**L1**)](PF_6), further ^{19}F and ^{31}P NMR spectroscopic data, and details of diffusion studies.

Acknowledgments

We gratefully acknowledge financial support from Natural Sciences and Engineering Research Council of Canada (Discovery Grant and Undergraduate Student Research Award), the Canada Foundation for Innovation, the Provincial Government of Newfoundland and Labrador and Memorial University. We thank Prof. Erika Merschod S. for access to a Leica DM 2500 microscope.

[1] a) S. Saffarzadeh-Matin, C. J. Chuck, F. M. Kerton, C. M. Rayner, *Organometallics* **2004**, *23*, 5176–5181; b) S. Saffarzadeh-Matin, F. M. Kerton, J. M. Lynam, C. M. Rayner, *Green Chem.* **2006**, *8*, 965–971; c) M. Herbert, A. Galindo, F. Montilla, *Organometallics* **2009**, *28*, 2855–2863; d) M. A. Grunlan, K. R. Regan, D. E. Bergbreiter, *Chem. Commun.* **2006**, 1715–1717; e) M. Herbert, F. Montilla, A. Galindo, *Polyhedron* **2010**, *29*, 3287–3293; f) M. Herbert, F. Montilla, A. Galindo, *Dalton Trans.* **2010**, *39*, 900–907; g) M. Herbert, F. Montilla, A. Galindo, *J. Mol. Catal. A Chem.* **2011**, *338*, 111–120; h) M. N. Missaghi, J. M. Galloway, H. H. Kung, *Organometallics* **2010**, *29*, 3769–3779; i) M. N. Missaghi, J. M. Galloway, H. H. Kung, *Appl. Catal. A* **2011**, *391*, 297–304.

[2] C.-F. Chow, S. Fujii, J.-M. Lehn, *Angew. Chem.* **2007**, *119*, 5095; *Angew. Chem. Int. Ed.* **2007**, *46*, 5007–5010.

[3] W. I. Dzik, S. E. Calvo, J. N. H. Reek, M. Lutz, M. A. Ciriano, C. Tejel, D. G. H. Hetterscheid, B. d. Bruin, *Organometallics* **2011**, *30*, 372–374.

[4] a) R. Chen, S. F. Mapolie, *J. Mol. Catal. A Chem.* **2003**, *193*, 33–40; b) C. R. Baar, M. C. Jennings, R. J. Puddephatt, *Organometallics* **2001**, *20*, 3459–3465; c) T. Irrgang, S. Keller, H. Maisel, W. Kretschmer, R. Kempe, *Eur. J. Inorg. Chem.* **2007**, 4221–4228; d) C. Bianchini, G. Giambastiani, L. Luconi, A. Meli, *Coord. Chem. Rev.* **2010**, *254*, 431–455.

[5] Z. Hu, F. M. Kerton, *Appl. Catal. A* **2012**, *413–414*, 332–339.

[6] a) G. C. Van Stein, G. Van Koten, K. Vrieze, C. Brevard, *Inorg. Chem.* **1984**, *23*, 4269–4278; b) S. Pal, S. Pal, *Polyhedron* **2003**, *22*, 867–873; c) M. G. B. Drew, M. R. S. Foreman, M. J. Hudson, K. F. Kennedy, *Inorg. Chim. Acta* **2004**, *357*, 4102–4112; d) S. Banerjee, J. Gangopadhyay, C.-Z. Lu, J.-T. Chen, A. Ghosh, *Eur. J. Inorg. Chem.* **2004**, 2533–2541; e) T. R. van den Ancker, G. W. V. Cave, C. L. Raston, *Green Chem.* **2006**, *8*, 50–53; f) X.-H. Zhou, T. Wu, D. Li, *Inorg. Chim. Acta* **2006**, *359*, 1442–1448; g) M. Habib, T. K. Karmakar, G. Aromi, J. Ribas-Arino, H.-K. Fun, S. Chantrapromma, S. K. Chandra, *Inorg. Chem.* **2008**, *47*, 4109–4117; h) I. I. Ebralidze, G. Leitus, L. J. W. Shimon, Y. Wang, S. Shaik, R. Neumann, *Inorg. Chim. Acta* **2009**, *362*, 4713–4720; i) N. C. Habermehl, P. M. Angus, N. L. Kilah, L. Norén, A. D. Rae, A. C. Willis, S. B. Wild, *Inorg. Chem.* **2006**, *45*, 1445–1462; j) P. K. Pal, S. Chowdhury, P. Purkayastha, D. A. Tocher, D. Datta, *Inorg. Chem. Commun.* **2000**, *3*, 585–589; k) D. Schultz, J. R. Nitschke, *Proc. Natl. Acad. Sci. USA* **2005**, *102*, 11191–11195.

[7] E. P. Maziarz III, X. M. Liu, E. T. Quinn, Y.-C. Lai, D. M. Ammon Jr, G. L. Grobe III, *J. Am. Soc. Mass Spectrom.* **2002**, *13*, 170–176.

[8] P. R. Andres, U. S. Schubert, *Macromol. Rapid Commun.* **2004**, *25*, 1371–1375.

[9] a) M. J. Kelso, H. N. Hoang, W. Oliver, N. Sokolenko, D. R. March, T. G. Appleton, D. P. Fairlie, *Angew. Chem.* **2003**, *115*, 437; *Angew. Chem. Int. Ed.* **2003**, *42*, 421–424; b) C. B. Smith, E. C. Constable, C. E. Housecroft, B. M. Kariuki, *Chem. Commun.* **2002**, 2068–2069; c) H. S. Chow, E. C. Constable, C. E. Housecroft, M. Neuburger, *Dalton Trans.* **2003**, 4568–4569.

[10] V. Amendola, L. Fabbrizzi, L. Gianelli, C. Maggi, C. Mangano, P. Pallavicini, M. Zema, *Inorg. Chem.* **2001**, *40*, 3579–3587.

[11] D. M. Haddleton, D. J. Duncalf, D. Kukulj, M. C. Crossman, S. G. Jackson, S. A. F. Bon, A. J. Clark, A. J. Shooter, *Eur. J. Inorg. Chem.* **1998**, 1799–1806.

[12] G. C. Van Stein, G. Van Koten, B. Debok, L. C. Taylor, K. Vrieze, C. Brevard, *Inorg. Chim. Acta* **1984**, *89*, 29–39.

[13] T. Sakurai, M. Kimura, A. Nakahara, *Bull. Chem. Soc. Jpn.* **1981**, *54*, 2976–2978.

[14] E. C. Constable, K. Harris, C. E. Housecroft, M. Neuburger, *Dalton Trans.* **2011**, *40*, 1524–1534.

[15] a) M. Valentini, H. Ruegger, P. S. Pregosin, *Helv. Chim. Acta* **2001**, *84*, 2833–2853; b) A. Macchioni, G. Ciancaleoni, C. Zuccaccia, D. Zuccaccia, *Chem. Soc. Rev.* **2008**, *37*, 479–489.

[16] H. B. T. Jeazet, K. Gloe, T. Doert, O. N. Kataeva, A. Jaeger, G. Geipel, G. Bernhard, B. Buechner, K. Gloe, *Chem. Commun.* **2010**, *46*, 2373–2375.

[17] a) M. Scheer, L. J. Gregoriades, M. Zabel, J. Bai, I. Krossing, G. Brunklaus, H. Eckert, *Chem. Eur. J.* **2008**, *14*, 282–295; b) R. V. Honeychuck, W. H. Hersh, *Inorg. Chem.* **1989**, *28*, 2869–2886.

[18] I. Avramov, *J. Non-Cryst. Solids* **2009**, *355*, 745–747.

[19] a) SHELX97: G. M. Sheldrick, *Acta Crystallogr., Sect. A* **2008**, *64*, 112–122; b) *DIRDIF99:* P. T. Beurskens, G. Admiraal, G. Beurskens, W. P. Bosman, R. de Gelder, R. Israel, J. M. M. Smits, *The DIRDIF-99 program system*, *Technical Report of the*

Crystallography Laboratory, University of Nijmegen, The Netherlands, **1999**; c) D. T. Cromer, J. T. Waber, *International Tables for X-ray Crystallography*, vol. IV, The Kynoch Press, Birmingham, England, Table 2.2 A, **1974**; d) J. A. Ibers, W. C. Hamilton, *Acta Crystallogr.* **1964**, *17*, 781; e) D. C. Creagh, E. W. J. McAuley *International Tables for Crystallography*, vol. C (Ed.: A. J. C. Wilson), Kluwer Academic Publishers, Boston, Table 4.2.6.8, pages 219–222, **1992**; f) D. C. Creagh, J. H. Hubbell *International Tables for Crystallography*, vol. C (Ed.: A. J. C. Wilson), Kluwer Academic Publishers, Boston, Table 4.2.4.3, pages 200–206, **1992**; g) CrystalStructure 3.7.0: *Crystal Structure Analysis Package*, Rigaku and Rigaku/MSC, **2000**–**2005**; h) CRYSTALS Issue 10: D. J. Watkin, C. K. Prout, J. R. Carruthers, P. W. Betteridge, *Chemical Crystallography Laboratory*, Oxford, UK, **1996**.

Received: December 19, 2011
Published Online: February 28, 2012

